# DISEASE MODELING USING INDUCED PLURIPOTENT STEM CELL DERIVATIVES

**PhD thesis**

**Tünde Berecz**

Basic and Translational Medicine Doctoral School

Semmelweis University

Supervisors: Ágota Apáti, PhD

Gábor Földes, MD, DSc

Official reviewers: Nándor Nagy, PhD

Tamás Bálint Csont, MD, PhD

Head of the Complex Examination Committee: Tivadar Tulassay, MD, Member of the Hungarian Academy of Sciences

Members of the Complex Examination Committee: Attila Patócs, MD, DSc

Péter Andréka, MD, PhD

Budapest

2023

# 1. Introduction

Human pluripotent stem cells and their differentiated derivatives provide promising opportunities for studying disease-related phenotypes *in vitro*. These approaches are particularly important when human cell types cannot be investigated directly or in the long-term, or no appropriate animal models are available. Studying differentiation and cell maturation processes can provide insights into disease development and lead us to identify possible targets for treatment. Cardiovascular and neurological diseases are the most common causes of death worldwide, strongly motivating the study of the cause and mechanisms leading to the development of these diseases. This thesis focuses on how to use human induced pluripotent stem cells (hiPSCs) and derivatives for disease modeling, especially when the disease affected cell types are hardly accessible such as cardiomyocytes or neural cell types.

## 1.1. Hippo pathway-YAP/TAZ signaling in doxorubicin induced cardiotoxicity

Anthracyclines are highly effective drugs particularly used against breast cancer and hematological malignancies. On the other hand, these drugs are the leading cause of cardiac dysfunction in cancer survivors. Since the regenerative potential of cardiac cells is known to be low, controlling cell survival in cardiomyocytes is more important than in cell types with greater regenerative capacity. Hippo signaling is an evolutionarily conserved pathway controlling organ size by regulating cell proliferation, apoptosis, and stem cell self-renewal. The key effectors of the Hippo pathway are Yes-associated protein (YAP) and transcriptional co-activator with PDZ-binding motif (TAZ). When YAP/TAZ is activated, it is translocated into the nucleus where it interacts with transcription factors as transcriptional co-activators promoting proliferation and inhibition of cell death. Dysregulation of the Hippo pathway, via activation of YAP and TAZ, results in uncontrolled proliferation and suppression of apoptosis in adult organs, and it has been implicated in tumorigenesis of breast, colon, lung, and liver cancers. Small molecule YAP inhibitors are a potential new therapeutic strategy for various cancers. Hippo pathway has also been shown to play a crucial role in regulating cardiomyocytes. In adult hearts, YAP silencing led to dilated cardiomyopathy and overexpression of YAP increased cardiomyocyte number and thus heart size in mouse models. Moreover, when YAP is overexpressed in the adult mouse heart, enhanced preservation of heart function and reduced scar size was observed after myocardial infarction. Consistent with the *in vivo* observation of doxorubicin-induced reduction of heart size in mice, doxorubicin treatment decreased the expression of YAP and caused cell death of neonatal and H9c2 rat cardiomyocytes

*in vitro*. In contrast, overexpression of YAP inhibited doxorubicin-induced cardiac cell loss *in vitro*. These findings suggest that YAP/TAZ activation is modified in response to doxorubicin treatment and is a promising potential target for regenerative or protective therapy of the heart. In this thesis, I present the first human-based study addressing Hippo pathway and YAP/TAZ transcriptional co-activators in doxorubicin-induced cardiotoxicity.

### 1.2. DiGeorge syndrome

DiGeorge syndrome/22q11.2 deletion syndrome, is the most common microdeletion syndrome with a prevalence of 1:3000 – 1:6000 in live births, affecting mainly the cardiovascular, nervous, and immune systems. The genetic background of the disease is a monoallelic microdeletion on chromosome 22 caused due to non-allelic homologous recombination. Hemizygosity of the affected genes leads to haploinsufficiency. Approximately 95 % of the cases are *de novo* deletions, and in 5 % of the cases is the disease inherited in an autosomal dominant manner. Deletions of different sizes can occur between low copy repeats on the 22q11.2 region. In over 90 % of the patients the typical 3 Mb long deletion if found affecting more than a hundred genes. 22q11.2 deletion causes a heterogeneous presentation of clinical symptoms, affecting several organ systems. The affected organ systems vary among patients, and the range of symptoms is broad, from mild to severe clinical manifestations. Notably, the highly variable phenotypic expression and severity of symptoms are not correlated with the size of the deletion, but severity usually increases when inherited. 22q11.2 deletion is one of the most common causes of congenital heart disease (CHD). Generating the appropriate animal model recapitulating all specific human features of the disease is difficult due to the different genetic organization of the locus and missing orthologue genes in mice. hiPSC-based models have the key advantage of providing the complicated genetic background of the disease and an unlimited resource for identifying the mechanisms underlying the pathology. In this thesis work hiPSCs were differentiated into cardiomyocytes and neural crest cells, as cardiac neural crest cells (cNCCs) also contribute to cardiovascular development and defects in cNCCs have been indicated to cause various cardiovascular disorders, including OFT anomalies, and VSD or TOF. However, the exact mechanisms of how improper NC development causes congenital heart defects are still not clearly understood.

### 1.3. Calcium signaling in hippocampal dentate gyrus granule cells

The dentate gyrus (DG) is the only known region of the human brain where neurogenesis persists into adulthood. New neurons generated in the DG are essential

for learning, pattern separation, and spatial memory formation, and alterations of hippocampal neurogenesis have been implicated in several disease conditions, including schizophrenia, epileptic seizures, Alzheimer's disease and depression. Since animal models are often inefficient in recapitulating human central nervous system (CNS) disorders, the generation of proper human cell-based systems has been proposed for both disease-modeling and drug screening purposes. Neurons differentiated from hPSCs using various protocols show characteristics of multiple neuronal subtypes. This heterogeneity can already be monitored at the progenitor state. A protocol has been developed to generate hPSC-derived neural progenitor cells (NPCs) that preferentially differentiate into a cell population enriched in hippocampal DG granule cells expressing Prospero Homeobox 1 (PROX1), a specific marker of this cell type. It was shown that directed differentiation to hippocampal granule neurons could reveal disease-related phenotypes in hiPSC models of schizophrenia and bipolar disorder.

Calcium ions, as ubiquitous intracellular messengers, play a fundamental role in numerous cellular processes, including proliferation, differentiation, and excitability. The measurement of neuronal calcium signaling has recently become an important tool to study calcium channel activity, intracellular calcium release, as well as calcium-dependent neurotransmitter release in *in vitro* cultured NPCs and neurons. We applied ATP, lysophosphatidic acid (LPA), and trypsin as ligands to evoke calcium signals in NPCs.

In neurons, cytoplasmic $Ca^{2+}$ originates both from internal $Ca^{2+}$ stores regulated by IP3R and RyR, and from the extracellular space primarily regulated by ligand-specific channels; such as glutamate receptors, or by voltage-gated $Ca^{2+}$ channels (VGCC). Granule neurons are excitatory glutamatergic neurons in the DG, therefore we studied spontaneous calcium gradients, and $Ca^{2+}$ signals induced by glutamate and depolarization agent KCl.

In this thesis work, we analyzed calcium signals of hiPSC-derived hippocampal DG granule NPC-s and neurons as functional characterization of these cell types.

## 2. Objectives

This thesis work aims to generate hiPSC-based in vitro models for better understanding cellular and molecular level disease mechanisms aiming to help the development of preventive strategies and treatment. Specifically, in this thesis, I present two disease models; i) a drug-induced disease and ii) a genetic disease.

Our previous RNA sequencing analysis of human myocardial samples of patients with doxorubicin-induced heart failure showed that YAP is an upstream regulator of differentially expressed genes. Several mechanisms in doxorubicin-induced cardiotoxicity have been reported in human cells, but there has been no human-based model studying the role of YAP/TAZ. In this study, by using hiPSC-derived cardiomyocytes (hiPSC-CMs), I aim to answer the following questions:

**1.** What is the mechanism for doxorubicin-induced cell death?
**2.** Is YAP/TAZ signaling altered by doxorubicin treatment?
**3.** Does modulation of YAP/TAZ affect cell functions?
**4.** Does modulation of YAP/TAZ affect doxorubicin-induced cell death?

The second part of this thesis work focuses on the discovery of mechanisms and developmental steps leading to the development DiGeorge syndrome, aiming to answer the following questions:

**1.** What are the in vitro phenotypes where DiGeorge hiPSC lines and their differentiated derivatives show differences as compared to control cells or to each other?

Finally, I present a method for studying calcium signaling in hiPSC-derived neural progenitor cells (hiPSC-NPCs), providing the basis for further studies of the neural aspects of DiGeorge syndrome, aiming to answer the following question:

**1.** How can intracellular calcium signaling be studied for functional characterization in hiPSC-NPCs not showing spontaneous calcium transients?

# 3. Results

## 3.1. Studying YAP/TAZ signaling in hiPSC-CMs for modeling doxorubicin induced cardiotoxicity

### 3.1.1. Doxorubicin induces YAP/TAZ nuclear translocation and cell death

hiPSC-CMs and an estrogen and progesterone receptor-positive human breast cancer cell line MCF7 were used to investigate the effects of chemotherapeutic drugs on cell death. 96 antineoplastic and cardiotherapeutic drugs were tested by using the FDA/EMA-approved Prestwick drug library (Fig. 1. A). High content screening showed that anthracycline agents, such as doxorubicin and daunorubicin, decreased cell viability (as shown by decreased mitochondrial membrane potential) and induced greater nuclear translocation of YAP/TAZ than other classes of drugs in both cell types. High TO-PRO-3 positivity (a marker of necrosis) was observed in response to doxorubicin in breast cancer cells but not in hiPSC-CMs (Fig. 1. A). Further exploring cell death in hiPSC-CMs, we found that hallmarks of apoptosis, such as activation of caspase 3/7, mitochondrial depolarization and nuclear fragmentation, were increased in response to doxorubicin exposure in a concentration-dependent manner (Fig. 1. B). However, necrosis was only induced in up to 7 % of hiPSC-CMs in response to 3 μM doxorubicin (Fig. 1. B).

### 3.1.2. Modulating YAP/TAZ expression and activation in hiPSC-CMs affects cell survival in doxorubicin treatment

YAP and TAZ mRNAs were expressed in hiPSC-CMs, as well as in human fetal heart tissue and adult ventricular cardiomyocytes, however, mRNA levels of YAP and TAZ were lower in *in vitro* differentiated hiPSC-CMs compared to those in human *ex vivo* samples (Fig. 2. A). YAP and TAZ are mechanotransducers, regulated by cell-extracellular matrix contacts and cell-cell contacts. Increases in cell density have been shown to decrease YAP and TAZ activity in other cell populations. To validate our cell culture model, we questioned whether cell density of hiPSC-CMs could affect YAP/TAZ expression and nuclear translocation. We found that YAP and TAZ mRNA levels were decreased in densely plated cells compared to sparsely plated cell populations (Fig. 2. B). YAP/TAZ nuclear translocation was also decreased in dense cultures (Fig. 2. B and C). These results corresponded with the known effects of mechanical cues on YAP and TAZ regulated by cell-cell connections.

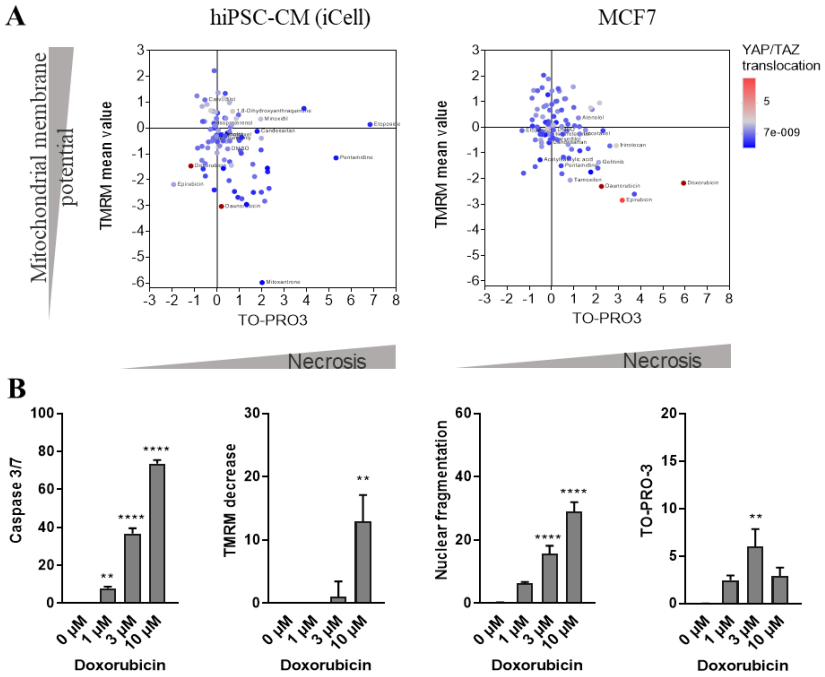


Figure 1. **YAP/TAZ activation and cell death profile of hiPSC-CM after drug treatment** (Find legend on next page.)

(**A**) YAP/TAZ activation is shown color coded in relation to necrosis as indicated by TO-PRO-3 staining and mitochondrial membrane potential (TMRM) levels in response to antineoplastic and cardiotherapeutic drugs in hiPSC-CMs and MCF7 cancer cells. Each dot represents an individual drug. (**B**) Changes in cell death markers in hiPSC-CM in response to increasing doxorubicin concentrations, percentage of positive cells is shown on the y axis (one-way ANOVA, ** $p<0.01$, **** $p<0.0001$, n=3).

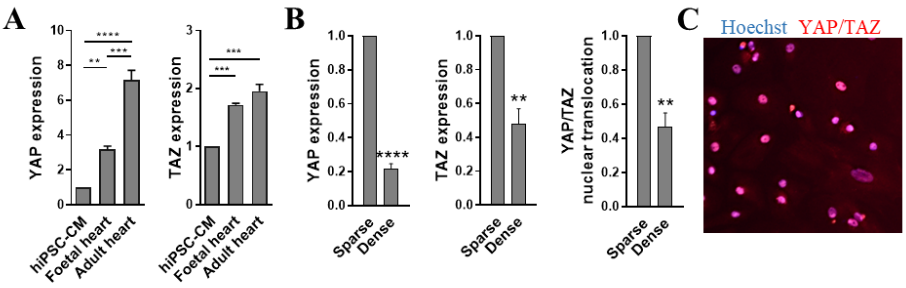


Figure 2. **Expression of YAP/TAZ**

(**A**) YAP and TAZ mRNA levels in hiPSC-CMs, fetal and adult heart (one-way ANOVA, ** $p<0.01$, *** $p<0.001$, **** $p<0.0001$, n=3). (**B**) mRNA expression of YAP and TAZ, and YAP/TAZ nuclear translocation in sparse and dense hiPSC-CM cell cultures (paired t-test, ** $p<0.01$, **** $p<0.0001$, n=3). (**C**) Immunocytochemistry of YAP/TAZ showing nuclear translocation of YAP/TAZ in control hiPSC-CMs.

Next, we investigated whether modulation of YAP and TAZ expression levels has an effect on cardiomyocyte function and doxorubicin-induced cell death. Transient silencing of both YAP and TAZ by siRNA resulted in a decrease in respective mRNA levels (Fig. 3. A). Transient overexpression of YAP by pEGFP-C3-hYAP1 plasmid nucleofection in hiPSC-CMs (Fig. 3. C) resulted in an over 8000-fold increase in mRNA levels compared to cells transfected with $GFP^+$ plasmid as control (Fig. 3. B). We next investigated whether YAP/TAZ gene silencing leads to modification of cardiac function by examining calcium transients as a hallmark of cardiomyocyte function using Fura-4F intracellular calcium indicator. Gene silencing did not affect calcium transient amplitude, time to peak or decay (Fig. 3. D). To note, calcium transient analysis with Fura-4F in YAP-overexpressing cells was not possible due to overlapping emission wavelength of Fura-4F and eGFP.

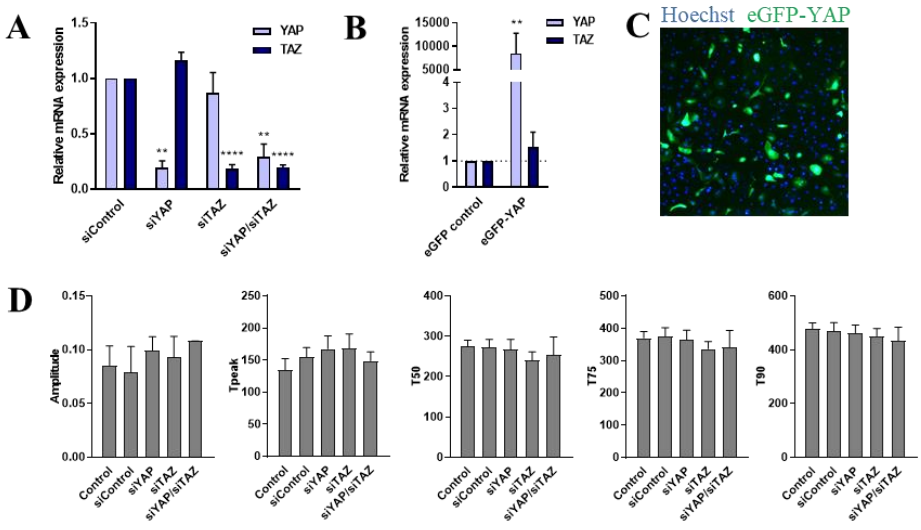


Figure 3. **Altered YAP/TAZ expression does not modulate calcium transient parameters in hiPSC-CMs**

(**A**) Silencing of YAP, TAZ or YAP/TAZ together and (**B**) overexpression of YAP in hiPSC-CMs. (**C**) Representative image showing eGFP-YAP expression in eGFP-YAP transfected hiPSC-CMs. (**D**) Calcium transient kinetics in YAP, TAZ or YAP/TAZ silenced hiPSC-CMs. (One-way ANOVA, ** $p<0.01$, **** $p<0.0001$, n=3).

Next, total cell count, necrosis marker TO-PRO-3 and mitochondrial membrane potential marker TMRM intensity were measured to assess the influence of YAP/TAZ modulation (silencing YAP and/or TAZ, or overexpression of YAP) on cell survival in doxorubicin treatment. High concentration of doxorubicin (15 µM) led to a significant decrease in cell number in hiPSC-CMs, and silencing YAP or TAZ, or YAP/TAZ together did not appear to influence this cellular phenotype (Fig. 4. A). In contrast, YAP overexpression resulted in increased cell number of untreated hiPSC-CMs. It decreased the level of cell loss in response to doxorubicin resulting in comparable total cell count to untreated control cells (Fig. 4. A). We found no significant difference between doxorubicin and vehicle-treated cells when measuring necrosis marker TO-PRO-3 (Fig. 4. B). On the other hand, decrease in mitochondrial membrane potential was more prominent in case of silencing YAP or YAP/TAZ compared to silencing TAZ only or siControl (Fig. 4. C), indicating that loss of YAP may further induce mitochondrial membrane potential loss after doxorubicin

treatment. In contrast to eGFP control cells, doxorubicin-induced mitochondrial membrane potential loss remained non-significant in YAP overexpressing hiPSC-CMs (Fig. 4. C).

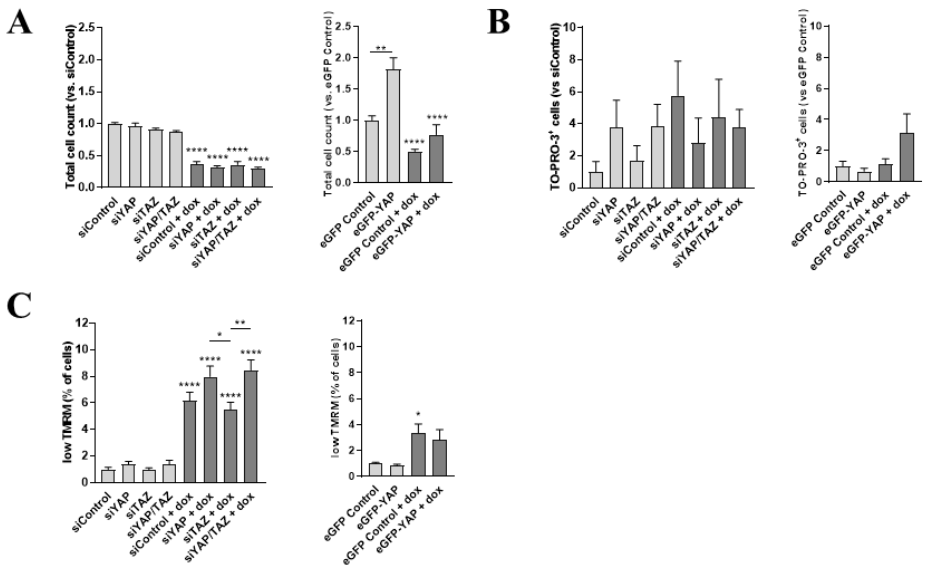


Figure 4. **YAP overexpression induces proliferation and inhibits doxorubicin-induced apoptosis hiPSC-CMs**

(**A**) Bar charts showing the effects of YAP, TAZ, or YAP/TAZ silencing or YAP-overexpression on cell number, (**B**) necrosis and **(C)** mitochondrial membrane potential in hiPSC-CMs in response to doxorubicin treatment.
(One-way ANOVA, * $p<0.05$, ** $p<0.01$, **** $p<0.0001$, n=3).

### 3.2. Modeling the cardiovascular features of DiGeorge syndrome

#### 3.2.1. Clinical description of human subjects involved in this study

A family with three DiGeorge patients from three generations (grandfather, mother and child) manifesting the disease with different severity, and two healthy relatives were involved in this study (Fig. 5.). Mild symptoms of the grandfather consist of articulation disorder and minimal facial dysmorphia. Moderate symptoms of the mother include vascular ring (surgically corrected in childhood), hypocalcemia and minimal facial dysmorphia. Symptoms of the child were severe and led to death at the age of 5 months; tetralogy of Fallot (ventricular septal defect, pulmonary atresia, right ventricular hypertrophy, misplaced aorta), atrial septal defect, asymmetric brain ventricles, hypocalcemia, hypoparathyroidism and minimal facial dysmorphia. The cause of death was cerebral herniation (shifting of cerebral tissue from its normal location into an adjacent space).

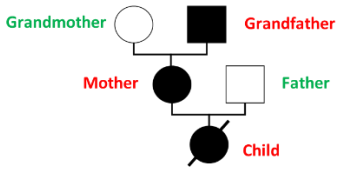


| |
|---|
| Grandmother ***Healthy control*** |
| Father ***Healthy control***<br>(Translocation between chromosomes 6 and 12) |
| Grandfather ***Patient with mild symptoms***<br>articulation disorder, minimal facial dysmorphia |
| Mother ***Patient with moderate symptoms***<br>hypocalcemia, vascular ring, minimal facial dysmorphia |
| Child ***Patient with severe symptoms***<br>Tetralogy of Fallot (ventricular septal defect, pulmonary atresia, right ventricular hypertrophy, misplaced aorta), atrial septal defect, asymmetric brain ventricles, hypocalcemia, hypoparathyroidism, minimal facial dysmorphia etc. |

Figure 5. **Pedigree of the family involved in the study**
Clinical symptoms of patients show increasing severity when the disease is inherited.

Karyotype testing of peripheral blood mononuclear cells (PBMCs) revealed chromosomal translocation between chromosomes 6 and 12 in the father. However, balanced translocations of this kind, when breakpoints are not in gene sequences or regulatory elements, usually do not cause phenotypic changes. The translocation was not inherited to the child. Considering that the father is a healthy individual, the breakpoint details were not further characterized.

#### 3.2.2. Generation and characterization of hiPSC lines

Reprogramming of PBMCs isolated from blood samples of all family members was performed by Sendai virus transduction. Pluripotency was verified by expression of pluripotency markers OCT4, NANOG and SSEA-4 (data not shown).

Karyotype testing showed no chromosomal alterations in hiPSC lines, with the exemption of the translocation between chromosomes 6 and 12 in hiPSCs of the father, later showed to be present in PBMCs, proving that it was not generated during reprogramming. The typical 3 Mb long deletion of the 22q11.2 region was verified by multiplex ligation-dependent probe amplification (MLPA) genetic test in hiPSC lines of all the three DiGeorge patients (data not shown).

### 3.2.3. Cardiac differentiation and characterization of cardiomyocytes

hiPSCs were differentiated into cardiomyocytes based on a previously described protocol. Immunostaining with the cardiac-specific marker TNNI3 showed high purity of cardiomyocytes in the cell culture on day 36 of differentiation (> 95%) (Fig. 5. A). This was further confirmed by mRNA expression analysis of multiple cardiac differentiation markers, with no difference between cell lines (Fig. 5. B.). The used differentiation protocol yields in a mixed population of cardiac subtypes, and cells thus express ventricular (MYL2), atrial (MYL7) and pacemaker (HCN4) markers.

Cardiac gap junction proteins (connexins) have been implicated to have a role in the development of cardiac anomalies, including TOF. Cx40 (GJA5) and Cx43 (GJA1) are two major gap junction proteins in the heart. Measurement of the expression of these two genes in cardiomyocytes showed a significantly lower level of GJA1 in the child's cells. In contrast, there was no difference observed in the expression of GJA5 (Fig. 5. C).

For functional characterization, analysis of intracellular calcium signals allows us to study calcium transient kinetics, depending on beating frequency. (Fig. 6. A-C). To test if *in vitro* phenotypes of cardiomyocyte function can be associated with patients with cardiovascular symptoms, hiPSC-CMs of mother and child were compared to the group of individuals without cardiovascular symptoms (controls and grandfather). No significant differences in frequency and calcium transient kinetics were observed in this case, suggesting that altered cardiomyocyte function is not the cause of cardiovascular symptoms in DiGeorge syndrome (Fig. 6. A-C).

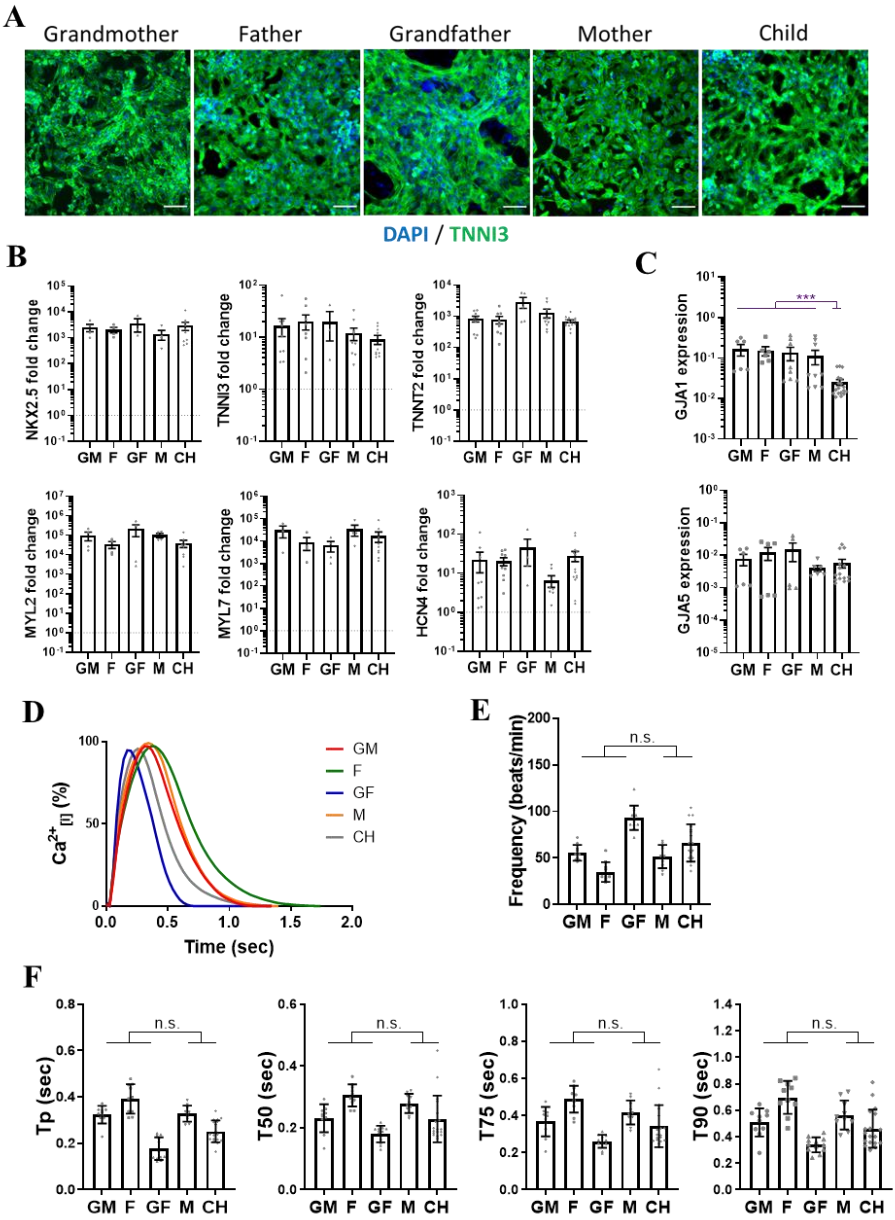


Figure 6. **Characterization of hiPSC-derived cardiomyocytes**
(Find legend on next page.)

(**A**) Immunostaining for cardiac marker TNNI3 on day 36 (scale bar: 100 mm). (**B**) mRNA expression measurements of cardiac differentiation markers on day 36, fold change compared to expression in respective hiPSCs (one-way ANOVA, non-significant, n=3). (**C**) mRNA levels of cardiac connexins and DiGeorge associated genes (unpaired t-test, *** $p<0.001$, n=3). (**D**) Intracellular calcium changes (mean values are shown for each cell line) and (**E**) frequency analysis on day 36 of cardiac differentiation. (**F**) Analysis of calcium kinetic parameters (Tp: time to peak, T50: 50 % decay, T75: 75 % decay, T90: 90 % decay). (Unpaired t-test, n.s. – non significant, n=3). (GM: grandmother, F: father, GF: grandfather, M: mother, CH: child).

### 3.2.4. Neural crest differentiation and characterization of neural crest spheroids and migratory neural crest cells

Most results presented in this chapter are preliminary, but principally show our approaches in the search for *in vitro* phenotypes. hiPSCs were differentiated into neural crest cells based on a previously described protocol. All cell lines produced migratory neural crest cells, however, immunostainings of neural crest markers SOX9 and AP2α showed significantly decreased intensity levels in NCCs of DiGeorge cell lines compared to controls (Fig. 7. A and B). Consistent with immunostaining results, mRNA expression levels of SOX9 and AP2α (TFAP2α) were decreased in DiGeorge cell lines compared to controls. Additionally, expression levels of another neural crest marker P75 (NGFR) in DiGeorge cells were also decreased compared to controls (Fig. 7. C). These results thus show that low expression of multiple neural crest markers is a characteristic of NCCs of DiGeorge patients and indicate a defective capacity to reach and maintain a proper specified neural crest state.

Next, we asked whether NCC function was changed in the migrating NCCs derived from DiGeorge syndrome patient cells. For this, we addressed cell growth. Growth curve based on viable cell counting showed a significantly decrease in cell number of hiPSC-NCCs of the mother and child compared to controls and grandfather (Fig. 7. D and E). Interestingly, the viable cell number of the grandfather was at the level of the controls with an obvious difference compared to the mother and child; The results show that hiPSC-NCC viability was affected in cells of DiGeorge patients with cardiovascular symptoms (mother and child) but was not altered in the cells of DiGeorge patient with no cardiovascular symptoms (grandfather). If this happens by cell death or decreased proliferation rate is under investigation.

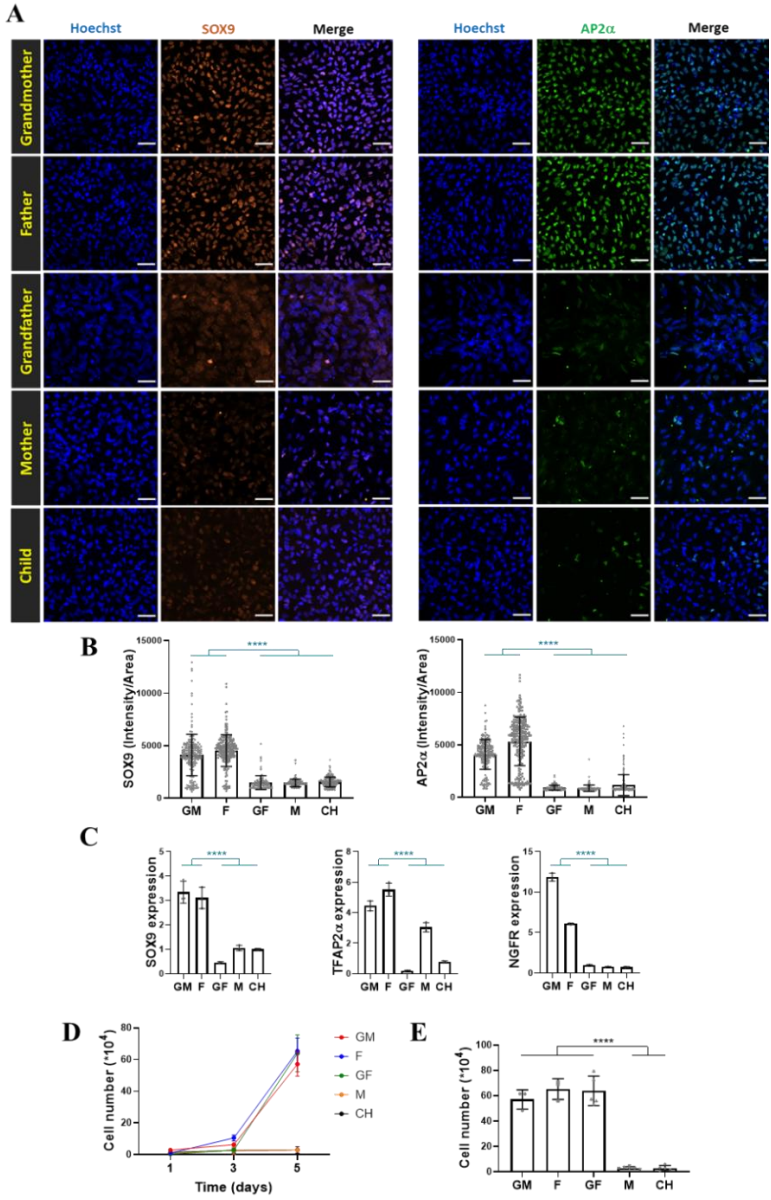


Figure 7. **Characterization of migratory neural crest cells**
(Find legend on next page.)

(**A**) Immunostainings for SOX9 and AP2α neural crest markers on migratory neural crest cells at passage 1 (scale bar: 50 mm). (**B**) Analysis of SOX9 and AP2α intensities in individual cells normalized to the size of nuclei. (**C**) mRNA expression measurements of neural crest markers on migratory neural crest cells at passage 1. (Unpaired t-test, **** $p<0.0001$, n=1). (**D**) Growth curve of passage 2 neural crest cells. (**E**) Analysis of viable cell number on day 5 after passaging (unpaired t-test, **** $p<0.0001$, n=3). (GM: grandmother, F: father, GF: grandfather, M: mother, CH: child).

### 3.3. Studying calcium signaling in hiPSC-derived hippocampal DG NPCs

Previous *in vitro* models for 22q11.2DS show that calcium handling is affected in neuronal differentiation of patient-derived hiPSCs. However, there has been no human-based report studying calcium signaling in hippocampal dentate gyrus granule cells in DiGeorge syndrome. For this aim, we developed techniques for studying calcium signaling in hiPSC-derived hippocampal NPCs and DG granule cells comparing a cytoplasmic $Ca^{2+}$ dye; Fluo-4 and a genetically encoded $Ca^{2+}$ indicator; GCaMP6. In this chapter, I representatively show our experiments with Fluo-4, being more suitable for our future experiments.

#### 3.3.1. Ligand-induced calcium signaling in hippocampal NPCs

As expected, neural progenitor cells did not show significant spontaneous calcium transients. For the investigation of their calcium homeostasis ATP, lysophosphatidic acid (LPA) and trypsin were applied as ligands to trigger calcium signals in the cells. Ionomycin $Ca^{2+}$ ionophore was applied to release $Ca^{2+}$ from intracellular stores. The intracellular calcium signal intensity triggered by ionomycin was set as the maximum $Ca^{2+}$ content of the cells and EGTA calcium chelator was applied to set the background (calcium-independent fluorescence) in our experiments. Approximately 12 % of the cells showed calcium response to ATP (Fig. 8. A) and nearly all the cells responded to trypsin (Fig. 8. B). The effect of these ligands was blocked when specific inhibitors were applied. Approximately 20 % of the cells showed calcium oscillations following ATP, LPA and trypsin treatment (Fig. 8. C), indicating the transmission of intracellular biological information.

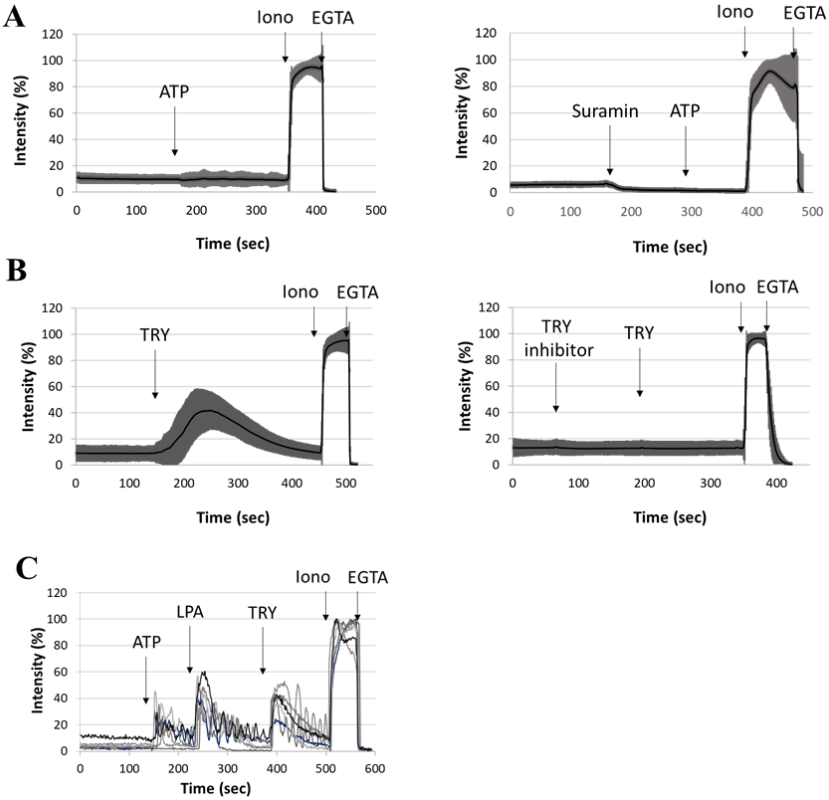


Figure 8. C**alcium signals evoked by ligands in hiPSC-derived hippocampal NPCs** (**A**) Calcium signals triggered by ATP are blocked by suramin P2 purinergic receptor inhibitor and (**B**) calcium signals triggered by trypsin are blocked by trypsin inhibitor in hiPSC-NPCs (Mean±SEM). (**C**) Calcium oscillations triggered by ATP, LPA and trypsin in individual hiPSC-NPCs.

The number of responding NPCs to glutamate neurotransmitter was highly variable between 20 to 80 % with relatively low signal intensity (Fig. 9. A) and hiPSC-NPCs did not show depolarization in response to KCl membrane depolarizing agent, proving the undifferentiated progenitor state of these cells. Finally, hiPSC-NPCs were further differentiated into neurons to test their differentiation capacity. In excitatory neurons, an action potential is followed by a calcium transient due to calcium influx. We tracked the emergence of spontaneous, rhythmic calcium activity after changing culture conditions and shifting NPCs from proliferation to differentiation and all the

cells responded to glutamate neurotransmitter (Fig. 9. B), showing the differentiation capacity of the NPCs into glutamatergic neurons.

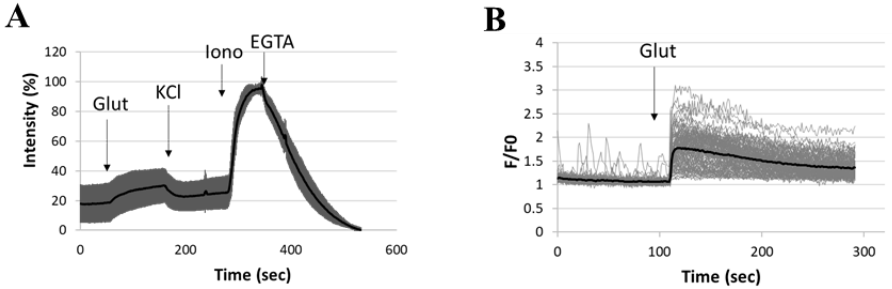


Figure 9. **Calcium signals in hiPSC-derived hippocampal NPCs and neurons**
(**A**) Calcium signals in response to glutamate and KCl in hiPSC-NPCs (Mean±SEM). (**B**) hiPSC-derived hippocampal DG neurons show spontaneous calcium transients and calcium response to glutamate.

## 4. Conclusions

The aim of this thesis work is to generate hiPSC-based *in vitro* models for better understanding cellular and molecular level disease mechanisms aiming to help the development of preventive strategies and treatment.

In the first model presented, the role of YAP/TAZ in doxorubicin-induced cardiotoxicity was investigated. We found that out of the tested 96 antineoplastic and cardiotherapeutic drugs, doxorubicin was the strongest inducer of YAP/TAZ nuclear translocation in both breast cancer cells and hiPSC-CMs, indicating that doxorubicin activates YAP/TAZ signaling. Doxorubicin-induced cell death was mediated by apoptosis, but not by necrosis in hiPSC-CMs. On the other hand, necrosis was induced in breast cancer cells as a result of doxorubicin treatment. YAP/TAZ expression and activation was decreased by increased cell density, corresponding with the mechanotransducer role of YAP/TAZ regulated by cell-ECM and cell–cell connections. Silencing YAP/TAZ did not alter calcium transients in hiPSC-CMs, indicating that YAP/TAZ does not regulate cardiomyocyte function. Overexpression of YAP rescued doxorubicin-induced cell loss by inhibiting apoptosis and through induction of proliferation in hiPSC-CMs. Based on our results, we conclude that cardio-selective increase of YAP expression could be a cardioprotective strategy during doxorubicin treatment of cancer patients.

In the second model, patient-derived hiPSCs were differentiated into relevant cell types to model the cardiovascular aspects of DiGeorge syndrome. We generated for the first time hiPSC lines for an inherited form of DiGeorge syndrome from three generations manifesting the disease with different severity with the typical 3 Mb deletion of the 22q11.2 chromosome region. We did not experience differences in expression of multiple cardiac differentiation markers and calcium transient analysis of hiPSC-CMs comparing patients with (mother and child) and without cardiovascular symptom (controls and grandfather. Cx43 (GJA1), a major gap junction protein in the heart showed significantly lower expression in hiPSC-CMs of the child. Based on these results we conclude that cardiomyocyte differentiation *per se* is not affected in DiGeorge syndrome, but structural development and molecular expression patterns in the heart can be involved in the mechanisms driving cardiovascular symptoms.

All cell lines were able to produce migratory NCCs, although decreased expression of multiple neural crest markers in cells of DiGeorge patients was observed allowing us to conclude that NCCs in DiGeorge syndrome are not able to develop normally. Additionally, impaired cell growth was observed in NCCs from DiGeorge patients with cardiovascular symptoms (mother and child). This indicates that decreased expression of neural crest markers combined with compromised cell growth of NCCs can be a factor leading to cardiovascular anomalies in DiGeorge syndrome.

Neurological disorders are frequent among DiGeorge patients with 30 % developing schizophrenia and 30-40 % developing autism spectrum disorder. Calcium deficit has been shown in cortical neurons differentiated from hiPSCs of 22q11.2DS patients. However, there has been no hiPSC-based study investigating hippocampal DG granule cells in patients with 22q11.2 deletion, despite that this region has been associated with many neurological conditions including schizophrenia and the involvement of these cells in 22q11.2DS has been shown in mice. To this aim, we have established an *in vitro* modeling system for studying calcium signaling in hiPSC-derived hippocampal NPCs, suitable to study NPC plasticity and potential disease related phenotypes. ATP, LPA and trypsin proved to be suitable for triggering calcium signals in hiPSC-NPCs and with a specific calibration method, characteristics of the triggered signal could be assessed. In our further experiments DiGeorge patient-derived and control cell lines will be studied accordingly. Additionally, ongoing RNA sequencing analysis of hiPSC lines and derivatives at multiple differentiation stages combined with CGH and WES data from the hiPSC lines aims to unfold the molecular and genetic background of *in vitro* phenotypes, giving us a basis for the association with the clinical manifestations.

**Publications related to the PhD thesis**

1. **Berecz T**, Yiu A, Vittay O, Orsolits B, Mioulane M, Dos Remedios CG, Ketteler R, Merkely B, Apati A, Harding SE, Hellen N, Foldes G. (2021) Transcriptional co-activators YAP1 TAZ of Hippo signalling in doxorubicin-induced cardiomyopathy. ESC Heart Fail, 9(1): 224-235. **IF: 4.411**

2. **Berecz T**, Husveth-Toth M, Mioulane M, Merkely B, Apati A, Foldes G. (2020) Generation and Analysis of Pluripotent Stem Cell-Derived Cardiomyocytes and Endothelial Cells for High Content Screening Purposes. Methods Mol Biol, 2150: 57-77.

3. Vofely G, **Berecz T**, Szabo E, Szebenyi K, Hathy E, Orban TI, Sarkadi B, Homolya L, Marchetto MC, Rethelyi JM, Apati A. (2018) Characterization of calcium signals in human induced pluripotent stem cell-derived dentate gyrus neuronal progenitors and mature neurons, stably expressing an advanced calcium indicator protein. Mol Cell Neurosci. 88: 222-230. **IF: 2.855**

**Other publications**

1. Izadifar M, **Berecz T**, Apati A, Nagy A. (2021) An Optical-Flow-Based Method to Quantify Dynamic Behavior of Human Pluripotent Stem Cell-Derived Cardiomyocytes in Disease Modeling Platforms. Methods Mol Biol. (doi: 10.1007/7651_2021_382)

2. Apati A, Varga N, **Berecz T**, Erdei Z, Homolya L, Sarkadi B. (2019) Application of human pluripotent stem cells and pluripotent stem cell-derived cellular models for assessing drug toxicity. Expert Opin Drug Metab Toxicol, 15(1): 61-75. **IF: 3.47**

3. Blacker TS, **Berecz T**, Duchen MR, Szabadkai G. (2017) Assessment of Cellular Redox State Using NAD(P)H Fluorescence Intensity and Lifetime. Bio Protoc, 7(2): e2105.

4. Tosatto A, Sommaggio R, Kummerow C, Bentham RB, Blacker TS, **Berecz T**, Duchen MR, Rosato A, Bogeski I, Szabadkai G, Rizzuto R, Mammucari C. (2016) The mitochondrial calcium uniporter regulates breast cancer progression via HIF-1alpha. EMBO Mol Med, 8: 569-585. **IF: 9,249**

5. Apati A, **Berecz T**, Sarkadi B. (2016) Calcium signaling in human pluripotent stem cells. Cell Calcium, 59: 117-123. **IF: 3.707**